CellPress

Cell Metabolism
Short Article

Obesity-Induced CerS6-Dependent $C_{16:0}$ Ceramide Production Promotes Weight Gain and Glucose Intolerance

Sarah M. Turpin,[1,2,8] Hayley T. Nicholls,[1,2,8] Diana M. Willmes,[1,2,8] Arnaud Mourier,[2,3] Susanne Brodesser,[2] Claudia M. Wunderlich,[1,2] Jan Mauer,[1,2] Elaine Xu,[1,2] Philipp Hammerschmidt,[1,2] Hella S. Brönneke,[1,2] Aleksandra Trifunovic,[2] Giuseppe LoSasso,[4] F. Thomas Wunderlich,[1,2] Jan-Wilhelm Kornfeld,[1,2] Matthias Blüher,[5] Martin Krönke,[2,6] and Jens C. Brüning[1,2,7,*]

[1]Max Planck Institute for Metabolism Research, Cologne, North Rhine-Westphalia 50931, Germany
[2]CECAD, Cologne, North Rhine-Westphalia 50931, Germany
[3]Max Planck Institute for the Biology of Aging, Cologne, North Rhine-Westphalia 50931, Germany
[4]Laboratory of Integrative and Systems Physiology, School of Life Sciences, École Polytechnique Fédérale, Lausanne 1015, Switzerland
[5]Department of Medicine, University of Leipzig, Leipzig, Saxony 04103, Germany
[6]Institute for Medical Microbiology, University Hospital Cologne, Cologne, North Rhine-Westphalia 50931, Germany
[7]Center for Endocrinology, Diabetes and Preventive Medicine (CEDP), University Hospital Cologne, Cologne, North Rhine-Westphalia 50931, Germany
[8]Co-first author
*Correspondence: bruening@nf.mpg.de
http://dx.doi.org/10.1016/j.cmet.2014.08.002

SUMMARY

Ceramides increase during obesity and promote insulin resistance. Ceramides vary in acyl-chain lengths from $C_{14:0}$ to $C_{30:0}$ and are synthesized by six ceramide synthase enzymes (CerS1–6). It remains unresolved whether obesity-associated alterations of specific CerSs and their defined acyl-chain length ceramides contribute to the manifestation of metabolic diseases. Here we reveal that *CERS6* mRNA expression and $C_{16:0}$ ceramides are elevated in adipose tissue of obese humans, and increased *CERS6* expression correlates with insulin resistance. Conversely, *CerS6*-deficient ($CerS6^{\Delta/\Delta}$) mice exhibit reduced $C_{16:0}$ ceramides and are protected from high-fat-diet-induced obesity and glucose intolerance. *CerS6* deletion increases energy expenditure and improves glucose tolerance, not only in $CerS6^{\Delta/\Delta}$ mice, but also in brown adipose tissue- ($CerS6^{\Delta BAT}$) and liver-specific ($CerS6^{\Delta LIVER}$) *CerS6* knockout mice. *CerS6* deficiency increases lipid utilization in BAT and liver. These experiments highlight CerS6 inhibition as a specific approach for the treatment of obesity and type 2 diabetes mellitus, circumventing the side effects of global ceramide synthesis inhibition.

INTRODUCTION

Ceramides are linked to obesity-associated metabolic dysfunction; however, the precise mechanism(s) of action remains poorly defined (Adams et al., 2004; Holland et al., 2007, 2011; Kolak et al., 2007). Pharmacological and genetic interventions that prevent de novo ceramide synthesis ameliorate many critical features of obesity-related diseases such as insulin resistance, atherosclerosis, and cardiomyopathy (Holland and Summers, 2008). Furthermore, it has been demonstrated that the potent antidiabetic actions of the adipokine, adiponectin, are partly attributed to adiponectin receptor-associated ceramidase activity, and consequent ceramide catabolism (Holland et al., 2011; Okada-Iwabu et al., 2013; Yamauchi et al., 2007). However, complete inhibition of sphingolipid and/or ceramide synthesis disrupts many cellular homeostatic and regulatory signaling pathways; therefore, targeting global de novo ceramide synthesis for the treatment of these diseases poses considerable risk of adverse effects (Holland et al., 2007).

Ceramides are at the center of sphingolipid metabolism, and are formed by the *N*-acylation of a sphingoid long-chain base. This reaction is regulated by individual (dihydro) ceramide synthases (CerSs), which are responsible for the generation of different acyl-chain ceramides ($C_{14:0}$–$C_{30:0}$) (Levy and Futerman, 2010). The recent generation of *CerS*-deficient mice has demonstrated that altering ceramide acyl-chain lengths via the manipulation of *CerS*s can have a broad range of functional and tissue-specific effects (Ginkel et al., 2012; Jennemann et al., 2012; Pewzner-Jung et al., 2010). For instance, *CerS1*-derived $C_{18:0}$ ceramides are essential for cerebellar development, whereas *CerS2*-derived $C_{22:0–24:0}$ ceramides regulate hepatic function, and *CerS3*-dependent > $C_{24:0}$ ceramides are crucial for maintaining skin barrier function (Ginkel et al., 2012; Jennemann et al., 2012; Pewzner-Jung et al., 2010). Thus, identifying the specific CerSs and consequently their derived acyl-chain ceramides that contribute to the development of obesity-associated insulin resistance may point toward specific therapeutic strategies for this common disease.

RESULTS AND DISCUSSION

CERS6 Expression Is Increased in Adipose Tissue of Obese Humans

Ceramide levels in the white adipose tissue (WAT), the skeletal muscle, and the liver are often elevated in obese humans and rodent models of obesity (Adams et al., 2004; Kotronen et al., 2010;

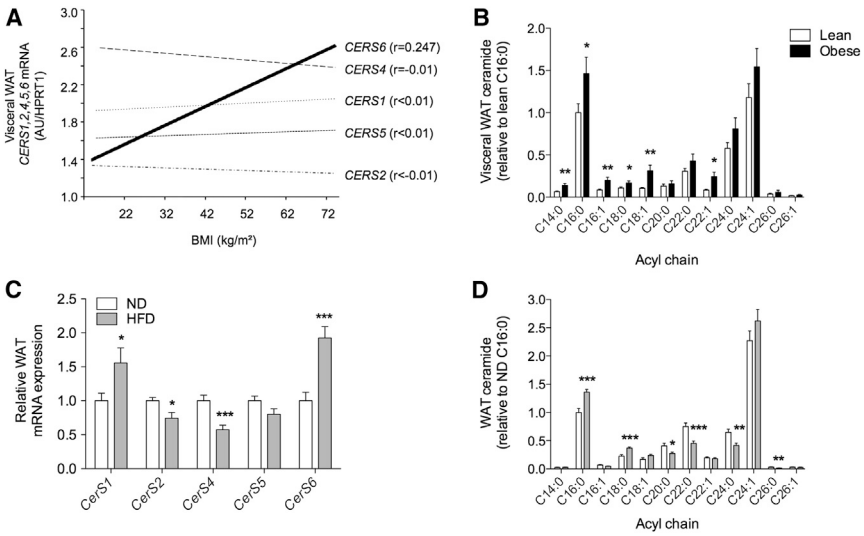

Figure 1. Expression of Ceramide Synthase 6 Is Positively Correlated with BMI

(A) Correlation between human ceramide synthase 1–6 (*CERS1–6*) gene expression and body mass index (BMI) in the visceral white adipose tissue (WAT) of human subjects (n = 439) normalized to hypoxanthine phosphoribosyltransferase 1 (*HPRT1*).

(B) Acyl-chain ceramides in visceral WAT of lean and obese subjects (n = 10/group).

(C) Gonadal WAT mRNA expression of *CerS*s in normal (ND)- and high-fat diet (HFD)-fed mice (n = 7 versus 8).

(D) Acyl-chain ceramides in the gonadal WAT of ND and HFD mice (n = 8/group). Values are expressed as mean ± SEM; *p < 0.05, **p < 0.01, ***p < 0.001 versus lean (B) or ND (C and D) as determined by unpaired Student's t test; r, Spearman's correlation coefficient. See also Figure S1 and Table S1.

Turinsky et al., 1990). However, a thorough analysis of the specific acyl-chain ceramides and expression profiling of the different CerSs in metabolically relevant tissues in obesity has not yet been conducted. Initially we sought to identify which *CERS*s and acyl-chain ceramides were altered in obese human subjects. Gene expression of *CERS1*, *2*, *4*, *5*, and *6* was determined in both visceral and subcutaneous WAT of 439 human subjects across a broad spectrum of body mass indices (BMIs). Only *CERS6* expression positively correlated with BMI, body fat content, and hyperglycemia, and negatively correlated with glucose infusion rate during euglycemic-hyperinsulinemic clamps (Figures 1A and S1A available online; Table S1). The positive correlation of *CERS6* mRNA expression in WAT with obesity and insulin resistance suggested that acyl-chain ceramide profiles could differ between lean and obese subjects. Indeed, in a smaller subcohort of 10 lean (BMI < 25 kg/m^2) versus 10 obese (BMI > 30 kg/m^2) subjects, $C_{14:0–18:1}$ and $C_{22:1}$ ceramides were increased (Figure 1B). Acyl-chain sphingomyelins, which are derived directly from ceramide, were also largely elevated in the obese, compared to lean, subjects (Figure S1B).

Similarly, mice fed a high-fat diet (HFD) showed increased *CerS6* and *1* expression, and correspondingly, $C_{16:0}$ and $C_{18:0}$ ceramides were significantly elevated (Figures 1C and 1D); however, sphingomyelin levels were not increased (Figure S1C). This indicates that upregulation of CerS6 expression and consequent increases in specific acyl-chain ceramides could represent a conserved phenomenon that contributes to both murine and human obesity; however, we cannot rule out that alterations in other complex sphingolipids could also contribute. Nonetheless, we proposed that disrupting individual CerSs could help to determine if a specific CerS(s) indeed plays a causal role in obesity development and associated negative metabolic consequences. Herein we have utilized the specificity of the CerS6 enzyme to selectively modulate the generation of $C_{16:0}$ ceramides.

Ablation of *CerS6* Protects from DIO and Glucose Intolerance

To elucidate the specific role of CerS6-dependent ceramide synthesis during obesity development, conventional *CerS6* knockout mice (*CerS6*$^{\Delta/\Delta}$) were generated via Cre-recombinase-mediated deletion of exon 4 in the *CerS6* gene, in the germline, that induced a frameshift and prevented translation of the highly conserved, catalytic longevity assurance domain (LAG1) (Figures S2A and S2B). *CerS6*$^{\Delta/\Delta}$ mice challenged with a HFD exhibited reduced $C_{16:0}$ ceramides in WAT, brown adipose tissue (BAT), and liver, but not in skeletal muscle (Figures 2A–2D). Strikingly, *CerS6*$^{\Delta/\Delta}$ mice were protected from diet-induced obesity (DIO), as evidenced by reduced body weight, decreased body fat content, reduced adipocyte size, and lower serum leptin concentrations compared to Control littermates (Figures 2E–2H). Similarly, *CerS6* deletion protected from macrophage infiltration and activation of proinflammatory gene expression in WAT of obese *CerS6*$^{\Delta/\Delta}$ mice (Figures 2I, 2J, and S2C). Indirect calorimetric analysis revealed that prevention of DIO might be attributed to an increased rate of energy expenditure (Figure 2K), as locomotor activity and food consumption were not different between *CerS6*$^{\Delta/\Delta}$ and Control mice (Figures S2D and S2E).

While total ceramide accumulation can contribute to insulin resistance in glucoregulatory tissues (Holland et al., 2007; Kotronen et al., 2010), it is still not known which CerSs are instigating these effects. As $C_{16:0}$ ceramides have been primarily implicated in the induction of insulin resistance in skeletal muscle, and $C_{16:0–18:0}$ ceramides have been linked to insulin resistance in the liver (Chavez and Summers, 2012), we investigated whether the deletion of *CerS6* could improve whole-body glucose metabolism. Indeed, HFD-fed *CerS6*$^{\Delta/\Delta}$ mice had significantly reduced serum insulin concentrations as well as improved glucose tolerance and insulin sensitivity compared to Control littermates (Figures 2L–2N). These improvements in glucose tolerance and insulin sensitivity were also observed in NCD-fed *CerS6*$^{\Delta/\Delta}$ mice whose body weight was only marginally lower than Controls (Figures S2F–S2H). Moreover, insulin-stimulated phosphorylation of protein kinase B/Akt, and its downstream target glycogen synthase kinase 3β (GSK3β) was improved in the liver, but not in skeletal muscle of HFD-fed *CerS6*$^{\Delta/\Delta}$ mice (Figures 2O and 2P). Collectively, the ablation of *CerS6* prevented DIO and glucose intolerance as well as obesity-associated WAT inflammation and improved insulin action in the livers of obese *CerS6*$^{\Delta/\Delta}$ mice.

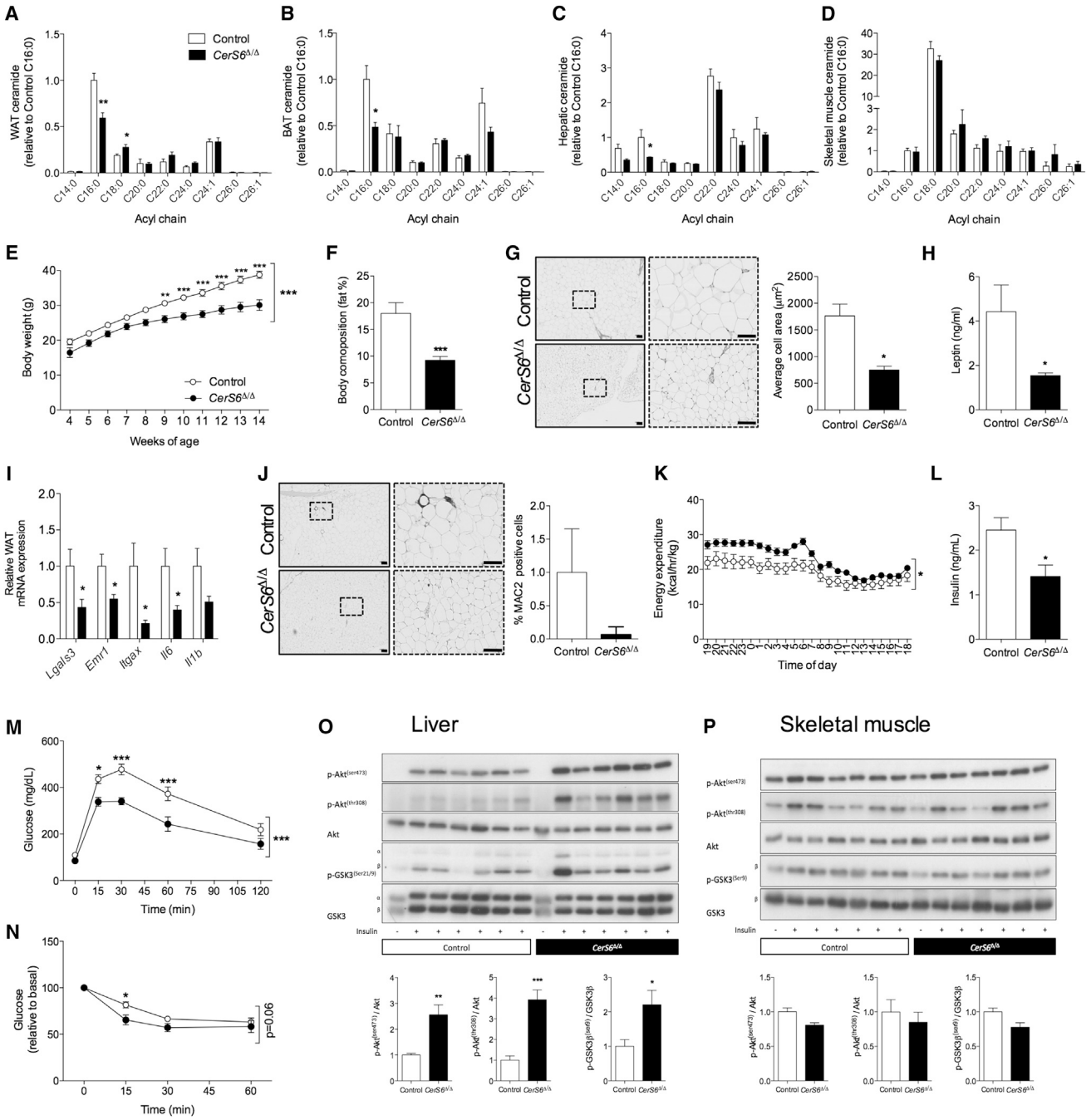

Figure 2. *CerS6* Deletion Protects from Diet-Induced Obesity and Improves Glucose Tolerance

(A–P) Analysis of high-fat diet (HFD)-fed *CerS6*$^{\Delta/\Delta}$ mice and Control littermates.

(A–D) Acyl-chain ceramides in the (A) gonadal white adipose tissue (WAT; n = 5/group), (B) brown adipose tissue (BAT; n = 5/group), (C) liver (n = 3/group), and (D) skeletal muscle (n = 6/group).

(E) Body weight (n = 12/group) and (F) percent body fat (n = 14/group).

(G) Representative images (scale bar, 100 μm) and quantification of adipocyte area in WAT (n = 3/group).

(H) Serum leptin (n = 6/group).

(I) mRNA expression of inflammatory markers in gonadal WAT (n = 7/group).

(J) Representative images (scale bar, 100 μm) and quantification of MAC2-positive cells in gonadal WAT (n = 6/group).

(K) Energy expenditure relative to lean body mass (n = 14 versus 29).

(L) Serum insulin (n = 8 versus 18).

(legend continued on next page)

Ablation of *CerS6*-Derived $C_{16:0}$ Ceramides in Myeloid Cells Fails to Protect from Obesity-Associated Glucose Intolerance

Next, we aimed to address in which tissues CerS6 acts to promote DIO and glucose intolerance. De novo synthesis of $C_{16:0}$ ceramides in macrophages has been shown to contribute to inflammasome activation and is suggested to be a key component of the signaling networks that connect lipid oversupply to inflammatory pathways and insulin resistance (Holland and Summers, 2008; Mitsutake et al., 2012; Schilling et al., 2013). Since $CerS6^{\Delta/\Delta}$ mice had less WAT proinflammatory macrophage infiltration, we sought to determine if myeloid cell-specific *CerS6* deletion ($CerS6^{\Delta MYEL}$) mice could improve the WAT inflammatory milieu and consequently prevent DIO and/or improve insulin sensitivity. To this end we crossed $CerS6^{loxP/loxP}$ mice with mice expressing Cre recombinase under the control of the lysozyme 2 gene (*Lyz2*) promoter/enhancer elements (LysMCre$^{+/-}$). Breeding $CerS6^{loxP/loxP}$*LysM*Cre$^{-/-}$ mice with $CerS6^{loxP/loxP}$ *LysM*Cre$^{+/-}$ mice produced mice with myeloid-specific *CerS6* deletion and littermate Controls (denoted as $CerS6^{\Delta MYEL}$ and Control, respectively). Despite reduced *CerS6* expression and reduced $C_{16:0}$ ceramides in macrophages, HFD-fed $CerS6^{\Delta MYEL}$ mice showed neither differences in body weight and adiposity, nor any improvements in glucose metabolism, compared to Control littermates (Figures S2I–S2P). Moreover, the expression of genes important and indicative of inflammatory and/or metabolic signaling in the WAT remained largely unchanged in these animals (Figure S2Q). These findings exclude the involvement of CerS6 in myeloid lineage-derived cells to alter whole-body glucose metabolism and indicate that the prevention of WAT inflammation in $CerS6^{\Delta/\Delta}$ mice occurs secondary to the prevention of obesity of conventional *CerS6*-deficient mice.

CerS6 Acts in BAT to Promote Adiposity and Glucose Intolerance

BAT oxidizes glucose and lipids primarily to produce energy that is dissipated as heat, and as such, is a highly active metabolic tissue (Bartelt et al., 2011). De novo ceramide synthesis has been shown to interfere with the ability of brown adipocytes to take up glucose (Fernández-Veledo et al., 2006), indicating that increased CerS expression and activity could negatively regulate BAT energy metabolism. Since increased BAT activity is associated with increased energy expenditure (Bartelt et al., 2011), we sought to determine if ablation of *CerS6* improved BAT function. Morphological analysis revealed a clear reduction in lipid droplet volume in BAT of HFD-fed $CerS6^{\Delta/\Delta}$ mice (Figure 3A). Stimulated triacylglycerol (TAG) release from ex vivo BAT sections of $CerS6^{\Delta/\Delta}$ mice was greater than that of Controls, suggestive of increased lipolysis in this tissue (Figure 3B). BAT mRNA analysis revealed significant increases in the expression of peroxisome proliferator-activated receptor gamma coactivator 1 alpha (*Pparg1ca*), nuclear respiratory factor 1 (*Nrf1*), and mitochondrial transcription factor A (*Tfam*) in $CerS6^{\Delta/\Delta}$ mice (Figure 3C). However, maximal respiratory chain enzymes' capacities in $CerS6^{\Delta/\Delta}$ BAT did not increase (Figure S3A). In agreement with the absence of increased mitochondrial biogenesis upon *CerS6* deletion, the maximal oxygen consumption rate assessed upon providing glycolytic substrates did not differ between the BAT of Control and $CerS6^{\Delta/\Delta}$ mice (Figure 3D). Interestingly, there was a significant elevation in mitochondrial β-oxidative capacity in isolated brown adipocytes from $CerS6^{\Delta/\Delta}$ mice compared to Controls (Figure 3E). Taken together, these findings suggest that deletion of CerS6 reduces lipid accumulation and improves BAT function through increased mitochondrial β-oxidative capacity.

To determine if increased BAT lipid oxidative capacity in $CerS6^{\Delta/\Delta}$ mice contributed to increasing energy expenditure, therefore protecting $CerS6^{\Delta/\Delta}$ mice from DIO, we deleted *CerS6* specifically in the brown adipocytes of mice. To this end, we engineered a bacterial artificial chromosome to express the Cre recombinase specifically in this tissue under control of the uncoupling protein (*Ucp*)-1 promoter, and which, upon injection in fertilized oocytes, yielded *Ucp1*Cre-transgenic mice (Figures S3B and S3C). Crossing *Ucp1*Cre mice with mice carrying a loxP-flanked *CerS6* allele yielded $CerS6^{flox/flox}Ucp1^{Cre/+}$, i.e., $CerS6^{\Delta BAT}$ mice. Despite a modest deletion efficiency of ~50%, which was highly restricted to BAT (Figure S3D), HFD-fed $CerS6^{\Delta BAT}$ mice exhibited reduced adiposity and increased energy expenditure despite no gross body weight differences (Figures 3F–3H). Similar to what was observed in conventional $CerS6^{\Delta/\Delta}$ mice, isolated brown adipocytes from $CerS6^{\Delta BAT}$ mice showed unaltered utilization of glycolytic substrates, but increased mitochondrial β-oxidative capacity (Figures 3I and 3J). $CerS6^{\Delta BAT}$ mice also demonstrated a modest improvement in glucose tolerance, but not insulin sensitivity (Figures 3K and 3L). While the partial deletion of *CerS6* specifically in the BAT expectedly did not fully recapitulate the profound metabolic improvements observed in $CerS6^{\Delta/\Delta}$ mice, these experiments illustrate that CerS6 may play a significant role in regulating BAT mitochondrial β-oxidative capacity to increase energy expenditure and improve systemic glucose homeostasis.

Hepatic *CerS6* Action Contributes to Diet-Induced Weight Gain and Glucose Intolerance

The liver is also a major site of lipid synthesis, storage, utilization, and export, as well as glucose metabolism. Deletion of key enzymes in the lipolysis, esterification, and fatty acid oxidation pathways can lead to dysregulation of lipid and glucose homeostasis in a variety of peripheral tissues (Girousse and Langin, 2012). Analysis of *CerS* expression in the livers of HFD mice demonstrated that only *CerS6* was upregulated with DIO, similar to what was observed in the adipose tissue of obese human subjects (Figure S4A). This coincided with increased $C_{14:0}$, $C_{16:0}$, $C_{18:0}$, $C_{20:0}$, and $C_{24:1}$ acyl-chain ceramides (Figure S4B), while in the livers of $CerS6^{\Delta/\Delta}$ mice, only $C_{14:0}$ and $C_{16:0}$ acyl-chain ceramides were selectively reduced (Figure 2C). Given the effect of *CerS6* deficiency on β-oxidative capacity in BAT, we aimed to elucidate whether the deletion of *CerS6* could also improve

(M) Glucose and (N) insulin tolerance tests (n = 9 versus 14).
(O and P) Representative immunoblots and quantifications of phosphorylated and total Akt and glycogen synthase kinase 3 (GSK3) in (O) liver and (P) skeletal muscle of insulin-stimulated (−/+) mice (n = 6/group). Values are expressed as mean ± SEM; *p < 0.05, **p < 0.01, ***p < 0.001 versus Control as determined by unpaired Student's t test (A–D, F–I, L, O, P) or two-way ANOVA (E, K, M, N). See also Figure S2.

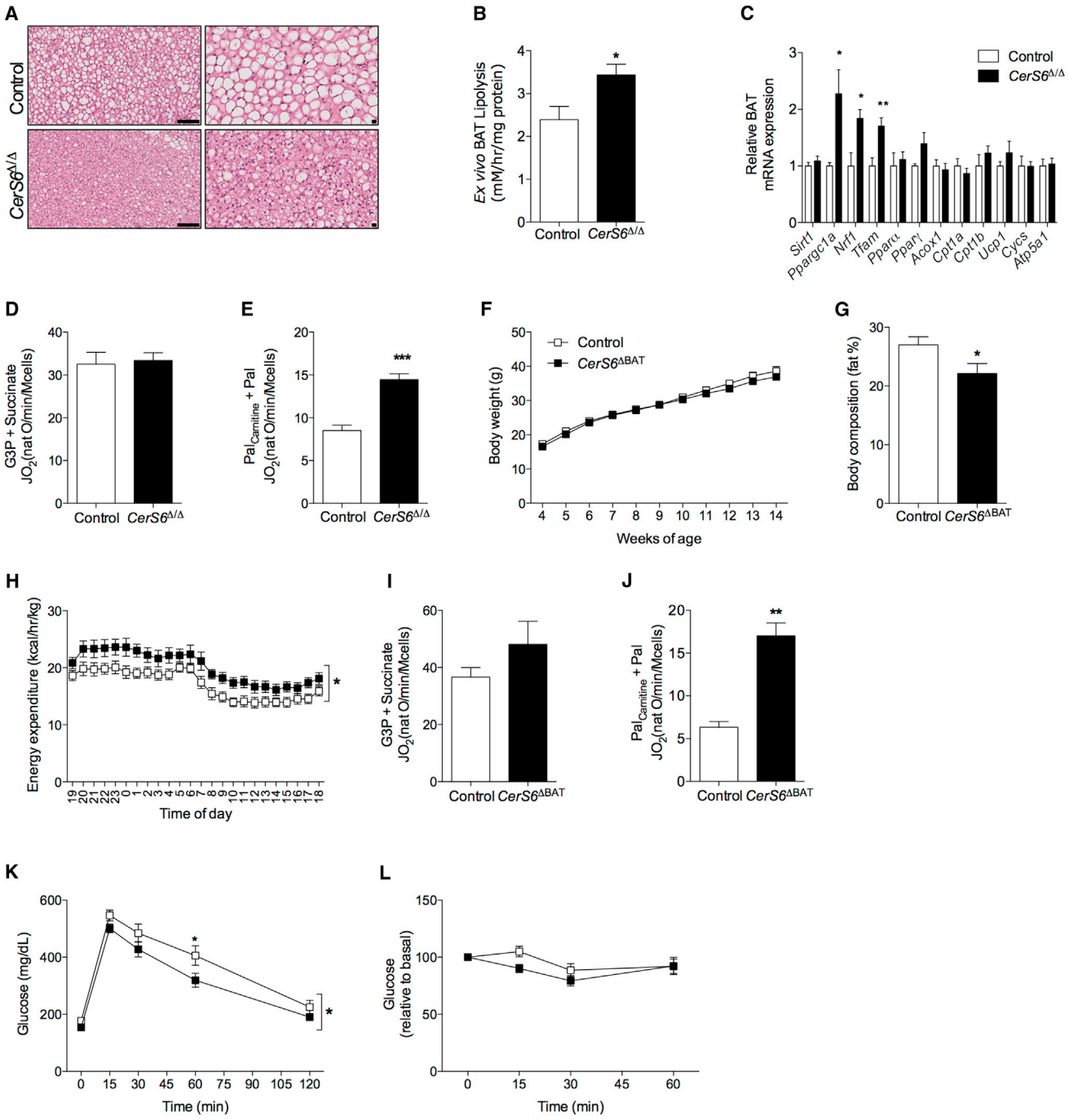

Figure 3. Deletion of *CerS6* Increases β-Oxidative Capacity in Brown Adipocytes

Analysis of high-fat diet (HFD)-fed (A–E) *CerS6*$^{\Delta/\Delta}$ mice, (F–L) *CerS6*$^{\Delta BAT}$ mice, and Control littermates.

(A) Hematoxylin and eosin stain of brown adipose tissue (BAT) sections (large scale bars, 100 μm; short scale bars, 10 μm) from HFD-fed Control and *CerS6*$^{\Delta/\Delta}$ mice.

(B) Triacylglycerol (TAG) release from BAT ex vivo (n = 8/group).

(C) mRNA expression of mitochondrial BAT functional regulators (n = 6/group).

(D and E) Mitochondrial oxygen consumption in response to (D) glucose-3-phosphate (G3P) and (E) palmitoylcarnitine ($Pal_{Carnitine}$) in brown adipocytes (n = 13/group).

(F) Body weight (n = 18/group), (G) percent body fat (n = 14/group), and (H) energy expenditure (n = 12/group) relative to lean body mass of HFD-fed Control and *CerS6*$^{\Delta BAT}$ mice. Mitochondrial oxygen consumption in response to (I) G3P and (J) $Pal_{Carnitine}$ in brown adipocytes from HFD-fed Control and *CerS6*$^{\Delta BAT}$ mice (n = 4/group). (K) Glucose (6 hr fast, n = 10 versus 12) and (L) insulin (1 U/kg, n = 20 versus 16) tolerance tests. Values are expressed as mean ± SEM; *p < 0.05, **p < 0.01 versus Control as determined by unpaired Student's t test (B, C, E, G, J) or two-way ANOVA (H, K, L). See also Figure S3.

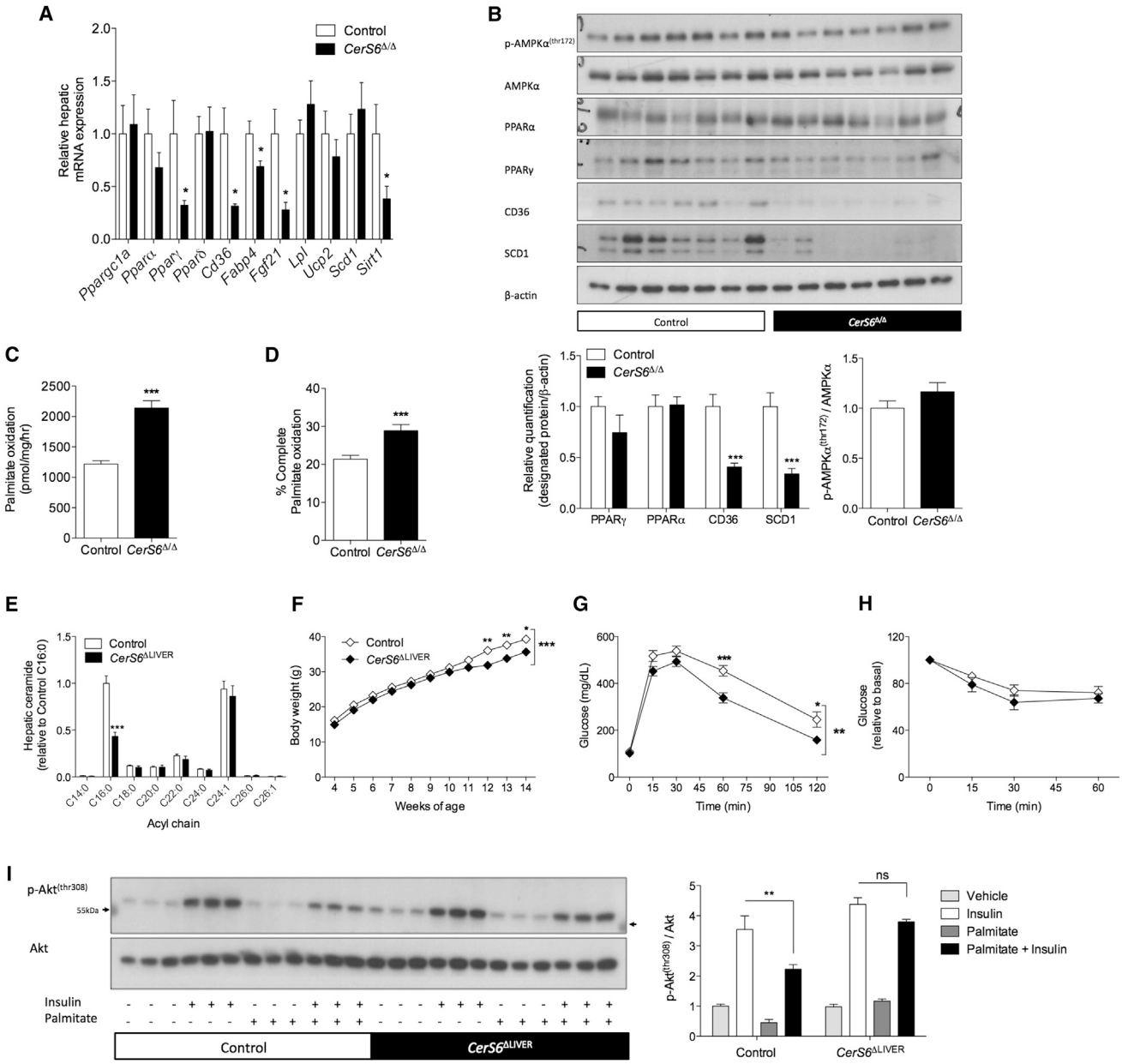

Figure 4. Hepatic Deletion of *CerS6* Increases Palmitate Oxidation and Improves Glucose Metabolism

Analysis of high-fat diet (HFD)-fed (A–D) *CerS6*$^{\Delta/\Delta}$ mice, (E–I) *CerS6*$^{\Delta LIVER}$ mice, and Control littermates.

(A) mRNA expression (n = 8/group) and (B) immunoblots and quantifications of functional metabolic regulators in the liver (n = 7/group).

(C) Palmitate oxidation and (D) percentage complete palmitate oxidation in primary hepatocytes (n = 8 versus 10 mice).

(E) Hepatic ceramide (n = 7 versus 5) and (F) body weight of HFD-fed Control and *CerS6*$^{\Delta LIVER}$ mice (n = 5 versus 7).

(G) Glucose (n = 12 versus 18) and (H) insulin (1 U/kg) tolerance tests (n = 7/group).

(I) Representative immunoblots and quantifications of phosphorylated and total Akt in primary hepatocytes, pretreated (−/+) with 0.5 mM palmitate for 6 hr, then insulin stimulated for 15 min (−/+); arrows indicate 55 kDa ladder (n = 6/group). Values are expressed as mean ± SEM; *p < 0.05, **p < 0.01 versus Control as determined by unpaired Student's t test (A–E) or two-way ANOVA (F–I). See also Figure S4.

hepatic lipid metabolism. Thus, we assessed both the mRNA and protein expression of key regulators of hepatic lipid metabolism in livers of Control and *CerS6*$^{\Delta/\Delta}$ mice. This analysis revealed a reduction of either mRNA and/or protein expression of the transcription factor peroxisome proliferator-activated receptor gamma (*Pparγ*) and its transcriptional targets, cluster of differentiation 36 (*Cd36*), fatty acid binding protein 4 (*Fabp4*), and stearoyl-CoA desaturase 1 (*Scd1*) in the livers of *CerS6*$^{\Delta/\Delta}$ mice independent of altered 5′ AMP-activated protein kinase phosphorylation (AMPK) (Figures 4A and 4B).

As PPARγ target genes control the uptake of lipids, and PPARγ has been suggested to regulate the storage of lipids in

hepatocytes, we examined the fatty acid oxidation rates in primary hepatocytes isolated from HFD-fed Control and *CerS6*$^{\Delta/\Delta}$ mice. The deletion of *CerS6* resulted in both more efficient and increased rates of palmitate oxidation (Figures 4C and 4D). To investigate potential mechanisms underlying these effects, we measured levels of fibroblast growth factor 21 (FGF21), which, through PPARα, increases hepatic lipid metabolism, and can also alter ceramide metabolism in an adiponectin-dependent manner (Holland et al., 2013). However, the mRNA expression of *Fgf21* in the liver was reduced, as were circulating levels of FGF21 in *CerS6*$^{\Delta/\Delta}$ mice (Figures 4A and S4C). Neither were there changes in PPARα, nor circulating high-molecular-weight adiponectin (Figures 4A, 4B, S4D, and S4E), which indicates that the elevated lipid oxidation in the livers of *CerS6*$^{\Delta/\Delta}$ mice occurs independently of FGF21 and adiponectin. Collectively, these experiments indicate that ablation of CerS6 and thus abrogating obesity-induced increases in CerS6 promotes β-oxidation both in the BAT and liver.

To further elucidate whether hepatic *CerS6* deficiency also contributes to the improved metabolism observed in *CerS6*$^{\Delta/\Delta}$ mice, we generated liver-specific *CerS6*-deficient mice (*CerS6*$^{\Delta LIVER}$). To this end, we crossed *CerS6*$^{loxP/loxP}$ mice with mice expressing Cre recombinase under the control of the mouse albumin enhancer and promoter and the mouse alpha-fetoprotein enhancers (*Alfp*Cre mice) (Kellendonk et al., 2000). Breeding *CerS6*$^{loxP/loxP}$*Alfp*Cre$^{-/-}$ mice with *CerS6*$^{loxP/loxP}$ *Alfp*Cre$^{+/-}$ mice produced mice with hepatocyte-specific *CerS6* deletion and littermate Controls (denoted as *CerS6*$^{\Delta LIVER}$ and Control, respectively). *CerS6*$^{\Delta LIVER}$ mice showed a selective reduction in both hepatic $C_{16:0}$ ceramides and dihydroceramides compared to Controls (Figures 4E, S4F, and S4G). While obese *CerS6*$^{\Delta LIVER}$ mice were only subtly protected from HFD-induced body weight gain (Figure 4F), the deletion of hepatic *CerS6* led to significantly improved glucose tolerance, but not insulin sensitivity, compared to Control littermates (Figures 4G and 4H). Furthermore, primary hepatocytes isolated from *CerS6*$^{\Delta LIVER}$ mice were protected from palmitate-induced reductions in insulin-stimulated Akt phosphorylation (Figure 4I), indicating that CerS6 is obligate for saturated fatty acid-induced hepatic insulin resistance. Taken together, our experiments highlight a specific causal role for CerS6, and consequently the generation of $C_{16:0}$ ceramides, in the development of obesity and glucose intolerance in mice and humans.

Conclusions

Herein we report a strong correlation, exclusively between *CerS6* expression in visceral and subcutaneous WAT of humans, with BMI and insulin resistance. Furthermore, we demonstrate that the main product of CerS6, $C_{16:0}$ ceramide, is also elevated in the visceral WAT of obese humans, as well as in WAT and liver of HFD-fed mice. These data are consistent with others who recently showed that $C_{16:0}$ ceramide in human subcutaneous adipose tissue correlates with HOMA-IR (Błachnio-Zabielska et al., 2012). In conjunction with the clear protection from obesity and improvement of insulin resistance and glucose tolerance in *CerS6*-deficient mice, these experiments indicate the specific importance of CerS6-derived $C_{16:0}$ ceramide in the pathogenesis of obesity and insulin resistance. Consistent with this notion, mice that are haploinsufficient for *CerS2*, thus resulting in a compensatory upregulation of $C_{16:0}$ ceramides, develop hepatosteatosis and insulin resistance (Raichur et al., 2014). While previous studies had revealed that either chemical inhibition or genetic manipulation of ceramide accumulation can alleviate insulin resistance both independent of and parallel with reduced adiposity (Boon et al., 2013; Holland et al., 2007; Turinsky et al., 1990; Ussher et al., 2010; Yang et al., 2009; Zhang et al., 2012), we demonstrate a critical role for distinct acyl-chain length specificity of ceramides in the development of both obesity and insulin resistance.

The first evidence of distinct and specific functions of CerS enzymes and their ceramide products stems from work in *C. elegans* (Menuz et al., 2009). Here the deletion of the CerS homolog *hyl-1* (catalyzing the synthesis of $C_{24:0–26:0}$ ceramides) decreased sensitivity to hypoxia, while deletion of *hyl-2* (catalyzing the synthesis of $C_{20:0–22:0}$ ceramides) increased hypoxia sensitivity (Menuz et al., 2009) in the absence of alterations in total ceramide levels. In conjunction with the generation of other specific *CerS* knockout mice (Ginkel et al., 2012; Jennemann et al., 2012; Pewzner-Jung et al., 2010), we further confirm the notion that CerSs and consequently their acyl-chain ceramide products have unique biological functions.

Specifically, we have identified *CerS6* as a negative regulator of β-oxidative capacity in the BAT and the liver. These effects, in contrast to Zigdon et al. (Zigdon et al., 2013), appear to be independent of increases in respiratory chain capacity. While we cannot exclude that CerS6 may be acting in other areas or discount the potential of developmental contributions of CerS6 deficiency, the generation of mice with specific deletion of *CerS6* in the BAT and liver clearly demonstrates that *CerS6* alters lipid utilization in these tissues.

In conclusion, we have identified a role for *CerS6* to modulate β-oxidation in BAT and liver to impair whole-body energy and glucose homeostasis in obesity. Hence, we provide evidence that a targeted pharmacological inhibition of *CerS6* could enable the generation of specific therapeutic approaches to combat obesity and type 2 diabetes mellitus and circumvent the potential adverse effects of blocking global ceramide synthesis.

EXPERIMENTAL PROCEDURES

Extensive experimental details can be found in Supplemental Experimental Procedures.

Human Subjects

The study was approved by the local ethics committee (Reg. No. 031-2006 and 017-12-23012012), and the participants gave their informed written consent.

Animal Care

All animal procedures were conducted in compliance with protocols approved by local government authorities (Bezirksregierung Köln) and were in accordance with NIH guidelines. Mice were allowed ad libitum access to food and water and maintained in a facility with a 12 hr light/dark cycle at 22°C–24°C.

Mouse Analysis

All experimental procedures were conducted using male mice as described below. Mice were placed on a HFD at weaning (i.e., 3 weeks of age). Body weight was assessed weekly from 3 to 15 weeks of age. ITT was conducted at 11 weeks, and GTT was conducted at 12 weeks. Between 15 and 18 weeks, mice were placed in metabolic chambers for calorimetric analysis. At

19 weeks, body composition was assessed prior to tissue and serum collection at 20 weeks of age.

Lipid Analysis

Sphingolipid levels were determined by liquid chromatography coupled to electrospray ionization tandem mass spectrometry (LC-ESI-MS/MS). Tissues were homogenized in water (10 mg of tissue per 100 μl) using the Precellys 24 Homogenizator (PEQLAB). Lipid extraction and LC-ESI-MS/MS analysis were performed as previously described (Schwamb et al., 2012). Samples were measured in duplicate.

Statistical Analysis

Data were analyzed for statistical significance using either Spearman's correlation coefficient, a two-way ANOVA with or without repeated measures, Bonferroni post hoc tests, or a two-tailed unpaired Student's t test as appropriate. p values less than 0.05 were considered statistically significant. All quantitative data are shown as the mean ± SEM.

SUPPLEMENTAL INFORMATION

Supplemental Information includes four figures, one table, and Supplemental Experimental Procedures and can be found with this article online at http://dx.doi.org/10.1016/j.cmet.2014.08.002.

AUTHOR CONTRIBUTIONS

S.M.T., H.T.N., and D.M.W. contributed equally to this work. J.C.B. and M.K. conceived the project. J.C.B., S.M.T., H.T.N., and D.M.W. designed the experiments, and S.M.T., H.T.N., and D.M.W. performed experiments and analyzed data. S.M.T., H.T.N., and J.C.B. wrote the manuscript. A.M. measured BAT respiration, S.B. conducted lipidomic analysis, M.B. analyzed human WAT, and J.-W.K. generated the *Ucp1*Cre-transgenic mice. The other authors also directly participated in the planning, execution, or analysis of the study. They also read and approved the final version of the submitted manuscript.

ACKNOWLEDGMENTS

We wish to thank Ayla Kap, Alexandra Kukat, Brigitte Hampel, Pia Scholl, Sigrid Irlenbusch, Esther Barth, and Jens Alber for technical assistance. This work was supported by the Leibniz Preis (BR1492/7-1 to J.C.B.), the Cologne Excellence Cluster on Cellular Stress Responses in Aging-Associated Diseases (CECAD; funded by the DFG within the Excellence Initiative by the German federal and state governments), the Helmholtz Alliance–Imaging and Curing Environmental Metabolic Diseases (ICEMED, Helmholtz Association), and the Center for Molecular Medicine Cologne (CMMC). S.M.T. was supported by the Alexander von Humboldt Foundation fellowship. G.L. is supported by an Outgoing AIRC/Marie Curie Fellowship. J.-W.K. was supported by the Emmy-Noether program (KO4728.1-1). P.H. was supported by the Köln Fortune Program. The research leading to these results has received funding from a cooperation agreement with Sanofi-Aventis, Deutschland GmbH.

Received: April 18, 2014
Revised: June 17, 2014
Accepted: July 25, 2014
Published: October 7, 2014

REFERENCES

Adams, J.M., II, Pratipanawatr, T., Berria, R., Wang, E., DeFronzo, R.A., Sullards, M.C., and Mandarino, L.J. (2004). Ceramide content is increased in skeletal muscle from obese insulin-resistant humans. Diabetes *53*, 25–31.

Bartelt, A., Bruns, O.T., Reimer, R., Hohenberg, H., Ittrich, H., Peldschus, K., Kaul, M.G., Tromsdorf, U.I., Weller, H., Waurisch, C., et al. (2011). Brown adipose tissue activity controls triglyceride clearance. Nat. Med. *17*, 200–205.

Błachnio-Zabielska, A.U., Baranowski, M., Hirnle, T., Zabielski, P., Lewczuk, A., Dmitruk, I., and Górski, J. (2012). Increased bioactive lipids content in human subcutaneous and epicardial fat tissue correlates with insulin resistance. Lipids *47*, 1131–1141.

Boon, J., Hoy, A.J., Stark, R., Brown, R.D., Meex, R.C., Henstridge, D.C., Schenk, S., Meikle, P.J., Horowitz, J.F., Kingwell, B.A., et al. (2013). Ceramides contained in LDL are elevated in type 2 diabetes and promote inflammation and skeletal muscle insulin resistance. Diabetes *62*, 401–410.

Chavez, J.A., and Summers, S.A. (2012). A ceramide-centric view of insulin resistance. Cell Metab. *15*, 585–594.

Fernández-Veledo, S., Hernandez, R., Teruel, T., Mas, J.A., Ros, M., and Lorenzo, M. (2006). Ceramide mediates TNF-alpha-induced insulin resistance on GLUT4 gene expression in brown adipocytes. Arch. Physiol. Biochem. *112*, 13–22.

Ginkel, C., Hartmann, D., vom Dorp, K., Zlomuzica, A., Farwanah, H., Eckhardt, M., Sandhoff, R., Degen, J., Rabionet, M., Dere, E., et al. (2012). Ablation of neuronal ceramide synthase 1 in mice decreases ganglioside levels and expression of myelin-associated glycoprotein in oligodendrocytes. J. Biol. Chem. *287*, 41888–41902.

Girousse, A., and Langin, D. (2012). Adipocyte lipases and lipid droplet-associated proteins: insight from transgenic mouse models. Int. J. Obes. (Lond.) *36*, 581–594.

Holland, W.L., and Summers, S.A. (2008). Sphingolipids, insulin resistance, and metabolic disease: new insights from in vivo manipulation of sphingolipid metabolism. Endocr. Rev. *29*, 381–402.

Holland, W.L., Brozinick, J.T., Wang, L.P., Hawkins, E.D., Sargent, K.M., Liu, Y., Narra, K., Hoehn, K.L., Knotts, T.A., Siesky, A., et al. (2007). Inhibition of ceramide synthesis ameliorates glucocorticoid-, saturated-fat-, and obesity-induced insulin resistance. Cell Metab. *5*, 167–179.

Holland, W.L., Miller, R.A., Wang, Z.V., Sun, K., Barth, B.M., Bui, H.H., Davis, K.E., Bikman, B.T., Halberg, N., Rutkowski, J.M., et al. (2011). Receptor-mediated activation of ceramidase activity initiates the pleiotropic actions of adiponectin. Nat. Med. *17*, 55–63.

Holland, W.L., Adams, A.C., Brozinick, J.T., Bui, H.H., Miyauchi, Y., Kusminski, C.M., Bauer, S.M., Wade, M., Singhal, E., Cheng, C.C., et al. (2013). An FGF21-adiponectin-ceramide axis controls energy expenditure and insulin action in mice. Cell Metab. *17*, 790–797.

Jennemann, R., Rabionet, M., Gorgas, K., Epstein, S., Dalpke, A., Rothermel, U., Bayerle, A., van der Hoeven, F., Imgrund, S., Kirsch, J., et al. (2012). Loss of ceramide synthase 3 causes lethal skin barrier disruption. Hum. Mol. Genet. *21*, 586–608.

Kellendonk, C., Opherk, C., Anlag, K., Schütz, G., and Tronche, F. (2000). Hepatocyte-specific expression of Cre recombinase. Genesis *26*, 151–153.

Kolak, M., Westerbacka, J., Velagapudi, V.R., Wågsäter, D., Yetukuri, L., Makkonen, J., Rissanen, A., Häkkinen, A.M., Lindell, M., Bergholm, R., et al. (2007). Adipose tissue inflammation and increased ceramide content characterize subjects with high liver fat content independent of obesity. Diabetes *56*, 1960–1968.

Kotronen, A., Seppänen-Laakso, T., Westerbacka, J., Kiviluoto, T., Arola, J., Ruskeepää, A.L., Yki-Järvinen, H., and Oresic, M. (2010). Comparison of lipid and fatty acid composition of the liver, subcutaneous and intra-abdominal adipose tissue, and serum. Obesity (Silver Spring) *18*, 937–944.

Levy, M., and Futerman, A.H. (2010). Mammalian ceramide synthases. IUBMB Life *62*, 347–356.

Menuz, V., Howell, K.S., Gentina, S., Epstein, S., Riezman, I., Fornallaz-Mulhauser, M., Hengartner, M.O., Gomez, M., Riezman, H., and Martinou, J.C. (2009). Protection of *C. elegans* from anoxia by HYL-2 ceramide synthase. Science *324*, 381–384.

Mitsutake, S., Date, T., Yokota, H., Sugiura, M., Kohama, T., and Igarashi, Y. (2012). Ceramide kinase deficiency improves diet-induced obesity and insulin resistance. FEBS Lett. *586*, 1300–1305.

Okada-Iwabu, M., Yamauchi, T., Iwabu, M., Honma, T., Hamagami, K., Matsuda, K., Yamaguchi, M., Tanabe, H., Kimura-Someya, T., Shirouzu, M., et al. (2013). A small-molecule AdipoR agonist for type 2 diabetes and short life in obesity. Nature *503*, 493–499.

Pewzner-Jung, Y., Park, H., Laviad, E.L., Silva, L.C., Lahiri, S., Stiban, J., Erez-Roman, R., Brügger, B., Sachsenheimer, T., Wieland, F., et al. (2010). A critical role for ceramide synthase 2 in liver homeostasis: I. alterations in lipid metabolic pathways. J. Biol. Chem. *285*, 10902–10910.

Raichur, S., Wang, S.T., Chan, P.W., Li, Y., Ching, J., Chaurasia, B., Dogra, S., Öhman, M.K., Takeda, K., Sugii, S., et al. (2014). CerS2 haploinsufficiency inhibits β-oxidation and confers susceptibility to diet-induced steatohepatitis and insulin resistance. Cell Metab. *20*, this issue, 687–695.

Schilling, J.D., Machkovech, H.M., He, L., Sidhu, R., Fujiwara, H., Weber, K., Ory, D.S., and Schaffer, J.E. (2013). Palmitate and lipopolysaccharide trigger synergistic ceramide production in primary macrophages. J. Biol. Chem. *288*, 2923–2932.

Schwamb, J., Feldhaus, V., Baumann, M., Patz, M., Brodesser, S., Brinker, R., Claasen, J., Pallasch, C.P., Hallek, M., Wendtner, C.M., and Frenzel, L.P. (2012). B-cell receptor triggers drug sensitivity of primary CLL cells by controlling glucosylation of ceramides. Blood *120*, 3978–3985.

Turinsky, J., O'Sullivan, D.M., and Bayly, B.P. (1990). 1,2-diacylglycerol and ceramide levels in insulin-resistant tissues of the rat in vivo. J. Biol. Chem. *265*, 16880–16885.

Ussher, J.R., Koves, T.R., Cadete, V.J., Zhang, L., Jaswal, J.S., Swyrd, S.J., Lopaschuk, D.G., Proctor, S.D., Keung, W., Muoio, D.M., and Lopaschuk, G.D. (2010). Inhibition of de novo ceramide synthesis reverses diet-induced insulin resistance and enhances whole-body oxygen consumption. Diabetes *59*, 2453–2464.

Yamauchi, T., Nio, Y., Maki, T., Kobayashi, M., Takazawa, T., Iwabu, M., Okada-Iwabu, M., Kawamoto, S., Kubota, N., Kubota, T., et al. (2007). Targeted disruption of AdipoR1 and AdipoR2 causes abrogation of adiponectin binding and metabolic actions. Nat. Med. *13*, 332–339.

Yang, G., Badeanlou, L., Bielawski, J., Roberts, A.J., Hannun, Y.A., and Samad, F. (2009). Central role of ceramide biosynthesis in body weight regulation, energy metabolism, and the metabolic syndrome. Am. J. Physiol. Endocrinol. Metab. *297*, E211–E224.

Zhang, Q.J., Holland, W.L., Wilson, L., Tanner, J.M., Kearns, D., Cahoon, J.M., Pettey, D., Losee, J., Duncan, B., Gale, D., et al. (2012). Ceramide mediates vascular dysfunction in diet-induced obesity by PP2A-mediated dephosphorylation of the eNOS-Akt complex. Diabetes *61*, 1848–1859.

Zigdon, H., Kogot-Levin, A., Park, J.W., Goldschmidt, R., Kelly, S., Merrill, A.H., Jr., Scherz, A., Pewzner-Jung, Y., Saada, A., and Futerman, A.H. (2013). Ablation of ceramide synthase 2 causes chronic oxidative stress due to disruption of the mitochondrial respiratory chain. J. Biol. Chem. *288*, 4947–4956.